Biophysical Journal Volume 65 November 1993 2124–2140

Energetics of Intermediates in Membrane Fusion: Comparison of Stalk and Inverted Micellar Intermediate Mechanisms

David P. Siegel
Miami Valley Laboratories, Procter & Gamble Company, Cincinnati, Ohio 45239-8707 USA

ABSTRACT To understand the mechanism of membrane fusion, we have to infer the sequence of structural transformations that occurs during the process. Here, it is shown how one can estimate the lipid composition-dependent free energies of intermediate structures of different geometries. One can then infer which fusion mechanism is the best explanation of observed behavior in different systems by selecting the mechanism that requires the least energy. The treatment involves no adjustable parameters. It includes contributions to the intermediate energy resulting from the presence of hydrophobic interstices within structures formed between apposed bilayers. Results of these calculations show that a modified form of the stalk mechanism proposed by others is a likely fusion mechanism in a wide range of lipid compositions, but a mechanism based on inverted micellar intermediates (IMIs) is not. This should be true even in the vicinity of the lamellar/inverted hexagonal phase transition, where IMI formation would be most facile. Another prediction of the calculations is that traces of apolar lipids (e.g., long-chain alkanes) in membranes should have a substantial influence on fusion rates in general. The same theoretical methods can be used to generate and refine mechanisms for protein-mediated fusion.

NOMENCLATURE

C_0	spontaneous curvature of a lipid monolayer
h	monolayer thickness
g_c	curvature elastic energy per unit area of monolayer (Eq. 1)
$g_{asv}(r)$	free energy required to produce an ASV between monolayers bent into radii equal to r (Eq. 8)
$g_{tsv}(r)$	free energy required to produce a unit length of TSV between monolayers bent into radii equal to r (Eq. 7)
G_c	total curvature elastic energy of an intermediate (Eq. 2)
k	Boltzmann's constant
k_G	Gaussian curvature elastic coefficient of a monolayer
k_m	bending elastic coefficient of a monolayer
R	axial radius of a stalk (see Fig. 2 *B*)
r	marginal radius of a stalk (see Fig. 2 *B*)
r_c	value of r for which the stalk-to-TMC transition is spontaneous (see Fig. 5)
r_3	radius of curvature of the dimpled monolayers in a TMC (see Fig. 2 *C*)
r_H	radius of monolayer curvature in the H_{II} phase
r_{TH}	radius of monolayer curvature in the H_{II} phase at T_H
T_H	equilibrium lamellar-to-inverted hexagonal (L_α/H_{II}) phase transition temperature
x	distance of the centroid of the TSV of a TMC from the axis of symmetry (see Fig. 2 *C*)
ϵ	marginal angle for stalk or IMI formation (see Fig. 2 *B*).

Received for publication 9 June 1993 and in final form 27 August 1993.

Address reprint requests to Dr. Siegel.

Abbreviations used: ASV, axially symmetric void (Fig. 1 *B*); DOPC, dioleoylphosphatidylcholine; DOPE, dioleoylphosphatidylethanolamine; DOPE-Me, *N*-mono-methylated dioleoylphosphatidylethanolamine; H_{II}, inverted hexagonal phase; ILA, interlamellar attachment (Fig. 3 *C*); IMI, inverted micellar intermediate (Fig. 3 *B*); L_α, liquid crystalline lamellar phase; PC, phosphatidylcholine; PE, phosphatidylethanolamine; PEG, polyethylene glycol; PS, phosphatidylserine; Q_{II}, inverted cubic phase; TMC, trans monolayer contact (Fig. 2 *C*); TSV, trilaterally symmetric void (Fig. 1 *C*).

0006-3495/93/11/2124/17 $2.00

INTRODUCTION

Little is known of the molecular mechanisms of membrane fusion in phospholipid membrane systems. Many researchers are seeking and characterizing proteins that mediate fusion in vivo (for recent reviews, see White (1992) and Bentz (1993)). Yet we may not be able to determine the mechanism of those proteins (or even determine whether catalysis of fusion per se is their role in vivo) until we understand what has to happen to apposed bilayers in order for them to fuse. If we understand the mechanisms of fusion in lipid systems, we can identify ways that proteins can catalyze similar processes under different circumstances, and what sort of protein structures would be most effective. We need to know the sorts of structural rearrangements that occur during fusion, and how they can be affected by lipid composition and other factors. Unfortunately, due to the highly transient and localized nature of the fusion process, we have little experimental data on fusion intermediate structures.

Therefore, it is important to use the best theoretical tools available to generate testable hypotheses about fusion mechanisms. Different mechanisms should be differently affected by lipid composition, ambient conditions, and other factors. It may be possible to infer the mechanisms at work by studying the influences of system composition and thermodynamic variables on the fusion rate. The results of recent experimental work on lamellar/inverted phase transitions have greatly improved our understanding of the relative stability of lipid structures of different geometries. The object of this work is to show how these advances can be used to identify and compare hypothetical fusion mechanisms and identify experimental tests that can distinguish between them. For instance, the research on nonlamellar phases has identified a previously unappreciated factor that should substantially affect the formation of fusion intermediates. This contribution, the free energy associated with the presence of hydrophobic interstices in intermediates, may underlie recent results concerning the effects of traces of hexadecane on the rate of fusion in anionic lipid systems (Walter et al., 1993).

Many fusion mechanisms and fusion intermediate structures have been proposed. The number and variety of proposals make it difficult to determine the genealogy of each idea. Generally, the proposals fall into two classes. The first is a mechanism in which the first interbilayer structure to form connecting the apposed (hereafter, *cis*) monolayers has a radius comparable to the length of a lipid molecule (e.g., Hui et al., 1982). The most detailed theoretical treatment of this class is that of Markin, Chernomordik and co-workers (Markin et al., 1984; Chernomordik et al., 1985, 1987; Leikin et al., 1987; Kozlov et al., 1989), in which this connection is a semi-toroidal structure termed a "stalk." The second class is based on inverted micellar intermediate (IMI) structures, as proposed by Verkleij and co-workers (Verkleij et al., 1980; Verkelij, 1984). Siegel (1984, 1986a, b, c) attempted a detailed kinetic theory of IMI-mediated fusion.

In the present work, the principal representatives of each of these classes are examined with the improved theoretical methods. The findings show that an IMI-based mechanism does not rationalize the observed fusion behavior of most lipid systems, including those near lamellar/inverted phase transitions. The results show that the stalk proposal of Markin, Chernomordik, and co-workers (Markin et al., 1984; Chernomordik et al., 1985, 1987; Leikin et al., 1987; Kozlov et al., 1989), in its original form, is also an unlikely fusion mechanism. However, modification of this insightful model (in light of more recent experimental data) yields a fusion mechanism that is compatible with the behavior of a wide variety of lipid systems. A modified stalk mechanism seems to require the least activation energy of any proposed mechanism involving the formation of continuous interfaces between apposed bilayers.

Elsewhere (manuscript in preparation), it will be shown that a lamellar/inverted phase transition mechanism based on stalks is also more compatible with observed behavior than a mechanism based on IMIs (Siegel, 1986a, b). The same theoretical methods that are used in this work can also be used to generate and refine hypotheses concerning the mechanism of fusion-catalyzing proteins. Using such methods, Siegel (1993) has argued that the mechanism of the fusion-catalyzing protein of influenza virus can be rationalized in terms of a stalk-based intermediate.

METHODS

A. Basic Assumptions

Formation of Discrete Intermediate Structures

Membrane fusion is the process by which two membranes and the aqueous compartments that they each enclose become continuous without leakage of the compartments. We assume that fusion occurs through formation of discrete intermediate structures with continuous lipid/water interfaces. Fusion appears to involve several very energy-intensive processes; e.g., the lipid/water interfaces have to be apposed to nearly molecular contact, the lipid/water interfaces must be disrupted, and hydrophobic regions of the membranes have to be brought into cohesion through the intervening aqueous region. Each of these processes can require energies of several kT or more per molecule (where k is Boltzmann's constant). In order to form a fusion pore, the structure of the membranes has to be altered across a patch with a radius at least equal to a bilayer thickness (4 nm), since this is the smallest continuous-bilayer connection that one can make between two membranes. (The process of hemifusion could require a smaller patch.) For most phospholipids, a patch this size contains ca. 300 lipid molecules. It is unlikely that a fusion pore is formed by a single catastrophic rearrangement involving energy-intensive perturbations to so many molecules, since the required activation energy would be prohibitively large. It is more likely that fusion occurs via formation of one or more discrete intermediate structures. Each intermediate could preserve some of the equilibrium structure of the original bilayers, and would require energy intensive perturbations to many fewer molecules in order to convert into the next intermediate in the sequence. Fusion could then occur in steps requiring lower activation energies, with much faster overall rates. The free energy of a intermediate with respect to the original bilayer structure is a lower-bound estimate of the free energy of activation required to form that intermediate.

The structures that require the smallest activation energies to form should be the most likely to occur. However, it is difficult to predict the actual rates of formation of hypothetical intermediates, even if one knows their energies. To do this, one needs detailed knowledge about the modes and frequencies of motion involved in intermediate formation. This approach has been used by the present author (Siegel, 1984, 1986a, b, c). Unfortunately, we have little data on the relevant modes and frequencies of motion in closely apposed membranes. There aren't even reliable ways of deciding which modes are involved. Even if we had this knowledge, it would still be difficult to calculate formation rates from the activation energies. Intermediate formation is likely to be a cooperative process, because large perturbations to the configuration of a given lipid molecule in a bilayer substantially change the energy required to make similar perturbations to its neighbors. Rate constants of cooperative processes do not have the simple activation energy dependence of Arrhenius rate constants. Therefore one cannot predict absolute rates of intermediate formation from estimates of the activation energy. However, reaction rates in general are strongly dependent on activation energies. Therefore we can qualitatively estimate the relative formation rates of different types of intermediates by comparing the intermediate energies.

Intermediate Energies

Intermediates are assumed to be structures with continuous lipid/water interfaces and no free monolayer or bilayer edges. The free energy of intermediate structures with respect to the planar bilayer is assumed to have only two components: the curvature elastic energy of the constituent lipid monolayers, and a free energy associated with the presence of hydrophobic interstices within the structure. Elegant studies by

Gruner, Parsegian, Rand, and others (for reviews, see Gruner (1989), Lindblom and Rilfors (1989), Seddon (1990), and Tate et al. (1991)) show that this two-component model is successful in rationalizing the relative stability of lamellar (L_α), inverted hexagonal (H_{II}), and inverted cubic (Q_{II}) phospholipid phases in excess water. The L_α, H_{II}, and Q_{II} phases are monolayer-based structures of very different geometries. The success of the model suggests that a similar approach is valid for continuous-monolayer intermediates in general. Gruner, Rand, Parsegian, and co-workers showed that a simple equation quantitatively describes the curvature energy of such assemblies (Gruner et al., 1986; Rand et al., 1990), even when the radius of the lipid/water interfaces is as small as 1 nm. Electrostatic effects are neglected. If only a small fraction of the lipids are charged, the ionic strength is high (e.g., 0.1 M), and the lipids are singly charged, then electrostatic effects are probably insignificant.

B. Calculations

Curvature elastic energies

The curvature free energy of the intermediates is evaluated by summing the curvature energies per unit area (g_c) of the constituent monolayer segments, using the equation (Helfrich, 1973)

$$g_c = \frac{k_m}{2}\left[\frac{1}{R_1} + \frac{1}{R_2} - C_0\right]^2, \qquad (1)$$

where k_m is the bending elastic coefficient of the monolayer, R_1 and R_2 are the principal radii of curvature in the region where g_c is evaluated, and C_0 is the spontaneous curvature of the monolayer. k_m and C_0 are constants determined by the lipid composition of the system, and can be measured by appropriate x-ray diffraction experiments (Rand et al., 1990). R_1, R_2, and C_0 are evaluated at the mid-surface of the monolayer. This is roughly the location of the neutral surface at which, to a good approximation, monolayer deformations can be described solely in terms of a bending elasticity, with minimal changes in area per molecule (Rand et al., 1990; Kozlov et al., 1991). The exact location of this neutral surface will change with lipid composition, but in general is near the monolayer mid-surface. The curvature free energy of a given area of monolayer with respect to an equivalent area of planar monolayer (R_1 and $R_2 = \infty$), G_c, is given by

$$G_c = \int_A g_c\, dA - \int_A \frac{k_m}{2} C_0^2\, dA, \qquad (2)$$

where the integrals are over the area evaluated at the monolayer midsurface. When an intermediate consists of contiguous monolayer regions with different geometries (and thus different values of g_c), the energies of the regions are evaluated separately and summed. In fact, there would be some exchange of lipid between these regions in a fashion tending to reduce the total energy, making this sum an overestimate.

The value of k_m is composition-dependent, but the values measured in inverted phase systems (e.g., Rand et al., 1990) and stable bilayers (e.g., Schneider et al., 1984; Bo and Waugh, 1989) are similar for a wide range of lipid compositions, ranging from egg phosphatidylcholine and 1-stearoyl, 2-oleoyl-phosphatidylcholine to dioleoylphosphatidylethanolamine (DOPE). The values are in the range $0.5–1.0 \times 10^{-19}$ J (k_m is one-half of the corresponding constant for bilayer deformation). In the following calculations, a value of 0.8×10^{-19} J will be used, which is close to the values determined for monolayers of DOPE and mixtures of DOPE and dioleoylphosphatidylcholine (DOPC) (Rand et al., 1990). We can use this average value to compare the energies of intermediates for a variety of lipid compositions.

The spontaneous curvature, C_0, is a sensitive function of the system composition and temperature. By convention, curvature that bends lipid monolayers around a water-containing region is negative in sign. Compositions stable in lamellar phases generally have either zero or slightly negative values of C_0. In the presence of excess water, DOPC has an equilibrium C_0 of about -0.1 nm^{-1} (Sjölund et al., 1989; Keller et al., 1993). Compositions that form H_{II} phases at equilibrium generally have C_0 values of ca. -0.3 nm^{-1} (Rand et al., 1990). Lipids that form H_{II} phases at high temperatures often form Q_{II} phases in a narrow range of lower temperatures (Gruner, 1989; Lindblom and Rilfors, 1989; Seddon, 1990; and Tate et al., 1991). The value of C_0 in systems with thermotropic L_α/inverted phase transitions generally decreases (becomes more negative) with increasing temperature (Tate et al., 1991; Gruner et al., 1988). The values of C_0 corresponding to Q_{II} phase formation in *N*-monomethylated dioleoylphosphatidylethanolamine (DOPE-Me) (Gruner et al., 1988; Siegel and Banschbach, 1990) appear to be ca.-0.2 to -0.3 nm^{-1}. A quantitative rationalization of this range will be discussed elsewhere (D. Siegel, manuscript in preparation).

In the calculations below, it will be assumed that the thickness of the lipid monolayer, h, is 1.8 nm and does not change as a function of curvature. The intermediate geometries are modeled as segments of spheres and regular circular toroids to simplify the mathematics. In practice, these surfaces might have more complex geometries.

The Gaussian curvature elastic energy of the intermediates is neglected, because the relevant Gaussian curvature elastic coefficient has not been measured for phospholipid systems. However, the effects of Gaussian curvature energies are probably small compared to the total energies of the intermediates, and do not affect the qualitative predictions made below. This is true as long as the absolute magnitude of the ratio of the Gaussian curvature elastic coefficient, k_G, to the mean curvature elastic coefficient, k_m, is small compared to unity. This ratio has been estimated in two lipid systems; a dialkyl glucolipid (Turner, 1990), and monololein (H. Chung and M. Caffrey, manuscript in preparation). The absolute magnitude of the ratio is ca. 0.1 in both cases. If the coefficients are in a similar ratio for phospholipids, then Gaussian curvature effects are not a major contribution. The Gaussian curvature elastic energy contribution for a structure can be determined by summing up the number of closed, orientable

monolayer surfaces of each genus (Andersson et al., 1988). The energy of a stalk forming between two liposomes would be lower than the energy of the two original liposomes by $4\pi k_G$. Stalks and TMCs (see below) would have the same Gaussian curvature energies. The Gaussian curvature energy of an IMI forming between two liposomes would be the same as the original two liposomes. Fusion pores (ILAs) would be lower in energy than the original two liposomes by $8\pi k_G$.

Hydrophobic interstice energies

To form intermediate structures between two membranes, the hydrophobic sides of the monolayers of the original bilayers have to peel apart over small areas. This creates hydrophobic interstices within the intermediate. Similar interstices occur in H_{II} phases (Turner and Gruner, 1992) as prismatic volumes between triplets of rod micelles (*stippled regions* in Fig. 1 *A*). Intermediates of different geometries will have hydrophobic interstices of different sizes and shapes. An interstitial volume of the same shape as found in the H_{II} phase will be referred to below as a *trilaterally symmetric void* (TSV) (e.g., Fig. 1 *B*).

Hydrophobic interstices are energetically unstable. If the interstices were vacuums, the surface tension at the interface between the methyl group surfaces of the monolayers and the vacuum would be close to the surface tension of hexadecane (ca. 27 mN/m (Small, 1986)). The energetic cost of creating such interface would be ca. 6.5 kT/nm^2. However, the actual energy of an interstice is determined in part by the response of the lipid molecules in the surrounding monolayers. The acyl chains of the lipids in the monolayers surrounding an interstice act to reduce the interstice surface area by stretching out to fill it (Kirk et al., 1984; Tate et al., 1987; Sjölund et al., 1987; Siegel et al., 1989b). When the chains stretch to nearly their fully extended length, the configurational entropy of the chains decreases, and the free energy increases. (It is possible that some other local change in phospholipid packing could account for interstice filling, and the interfaces of the monolayers of the H_{II} phase also distort slightly so as to aid this process; see Turner and Gruner, 1992.) Therefore, the net increase in free energy associated with the presence of a hydrophobic interstice depends on the size and geometry of the interstice, and on the properties of the surrounding lipid molecules. Unfortunately, no accurate molecular-level theory of these energies exists.

However, the interstice energy can be estimated by analysis of the free energy differences between L_α and H_{II} phases. The L_α/H_{II} transition is driven by a reduction in curvature energy, while the free energy penalty associated with producing the two prisms of TSV in the H_{II} unit cell tends to oppose the transition (Gruner, 1989; Lindblom and Rilfors, 1989; Seddon, 1990; and Tate et al., 1991). The transition occurs when the magnitudes of these two free energy contributions are equal. The magnitude of the curvature energy contribution at the phase transition can be calculated, using data from x-ray diffraction studies of the H_{II} phase. This yields the free energy needed to stabilize a unit length of TSV in the H_{II} phase. We can differentiate the resulting expression for the total energy with respect to the radius of curvature to estimate how the energy changes for TSVs of different cross-sectional area.

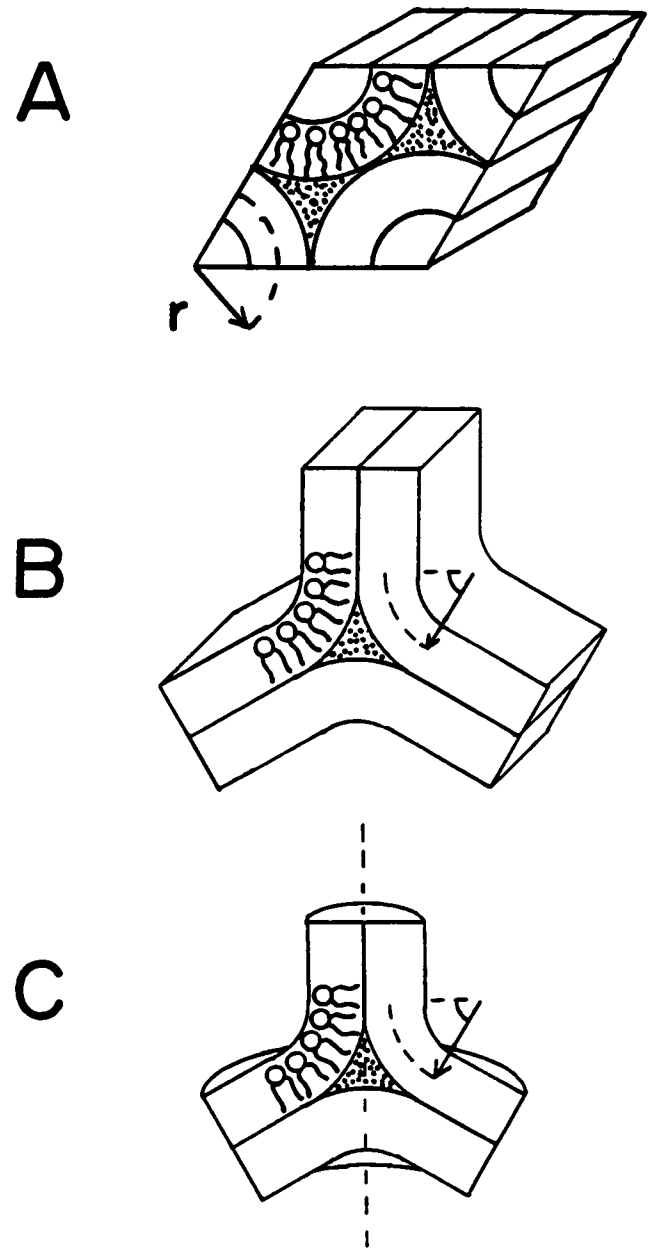

FIGURE 1 (*A*) TSVs in a unit cell of inverted hexagonal (H_{II}) phase, shown as stippled areas. *r* is the radius of curvature of the monolayers at the margin of the TSV. (*B*) TSV as it would exist at the junction of three bilayers. (*C*) ASV formed at the juncture of a rod micelle and a bilayer, or at the base of a stalk (Fig. 2 *B*). The ASV (*stippled*) is cylindrically symmetric about the dashed vertical axis.

Let r_H be the radius of the monolayer tubes in the H_{II} phase in excess water at an arbitrary temperature, evaluated at the monolayer midsurface. Let $g_{tsv}(r_H)$ be the free energy of a unit length of TSV, which is a function of r_H. The total free energy, *G*, of a unit cell of H_{II} phase of length *L* compared to an equivalent area of planar L_α phase monolayer is the sum

of the curvature and interstice energies;

$$G = \pi k_m r_H L[(-1/r_H - C_0)^2 - C_0^2] + 2Lg_{tsv}(r_H). \quad (3)$$

At the equilibrium L_α/H_{II} phase transition temperature, T_H, the value of r_H is r_{TH}. It is assumed that the net curvature in the H_{II} phase at T_H ($-1/r_{TH}$) is equal to C_0: this is true to within a couple of percent (Rand et al., 1990). At T_H, the free energies of lipid in L_α and H_{II} phases are equal; so the two terms in Eq. 3 must be equal in magnitude and opposite in sign. Equating them, one obtains an expression for g_{tsv} at $r_H = r_{TH}$,

$$g_{tsv} = \pi k_m/(2r_{TH}). \quad (4)$$

To estimate the dependence of g_{tsv} on the radius of curvature, r_H, of the monolayers bounding the interstitial space, one first differentiates Eq. 3 with respect to r_H, keeping the monolayer area constant. The constant-area constraint makes L a function of r_H ($dL/dr_H = -L/r_H$). Differentiating Eq. 3 with respect to r_H, then setting $r_H = r_{TH} = -1/C_0$, one obtains

$$\frac{dG}{dr_H} = \left(-\frac{2L}{r_H}\right)g_{tsv}(r_H) + 2L\left(\frac{dg_{tsv}(r_H)}{dr_H}\right). \quad (5)$$

Structural stability of the H_{II} phase requires that $dG/dr_H = 0$ at $r_H = r_{TH}$, so

$$dg_{tsv}/dr_H = g_{tsv}/r_{TH}, \quad (6)$$

for $r_H = r_{TH}$.

For small departures of r_H from r_{TH},

$$g_{tsv}(r_H) = g_{tsv}(r_H = r_{TH}) + \frac{dg_{tsv}(r_H = r_{TH})}{dr_H}(r_H - r_{TH})$$

$$= \pi k_m \frac{r_H}{2r_{TH}^2}. \quad (7)$$

For $k_m = 8.5 \times 10^{-20}$ J and $r_{TH} = 3.09$ nm (r_H for DOPE at 22°C (Rand et al., 1990)), $g_{tsv} = 4.32 \times 10^{-11}$ J/m, or 10.5 kT/nm of TSV length at around room temperature. T_H for DOPE is 5–10°C (Gruner et al., 1988), and hence r_{TH} is in fact slightly different than the value of r_H at 22°C. However, the values obtained at 22°C by Rand et al. (1990) represent the most accurate measurements made with C_0 evaluated near the neutral surface of the monolayer. Hence, these values will be used, tolerating the small error incurred. Eq. 7 yields the free energy of creating a TSV of unit length between three monolayers that are each bent into a given radius of curvature.

An interstice of another shape is depicted in Fig. 1 *C*. This interstice is cylindrically symmetric about the vertical axis, and is referred to as an *axially symmetric void* (ASV). The difference in geometry relative to a TSV may mean that the modes by which adjacent acyl chains stabilize this interstice are different. However, we do not know which modes are involved, or their geometry dependence. The magnitude of the interstice energy is determined by the fraction of the volume of the interstice that can be filled by configurational changes in adjacent lipid chains. The volume that can be filled is the product of the number of chains that border the interstice (proportional to its surface area) and the average length to which they can stretch. At present, we do not know how changes in one of these factors affects the other. Therefore, we make the simplest assumption, which is that the same free energy *per unit of total interstice volume* is required to form an ASV as is required to form a TSV of unit length. One then finds that the free energy needed to form an interstice of this geometry, surrounded with monolayers bent into a radius of curvature r, is

$$g_{asv} \approx 0.354\,(r + h/2)g_{tsv}(r), \quad (8)$$

where h is the lipid monolayer thickness (Fig. 1 *C*). For $r = r_{TH} = 3.09$ nm and $h = 1.8$ nm, g_{asv} is 6.1×10^{-20} J or ca. 15 kT.

Eq. 7 yields g_{tsv} for a lipid composition forming an H_{II} phase with the measured values of k_m and r_{TH}. This is designated as the reference system. However, this equation can be used to calculate the free energy of hydrophobic interstices of this geometry in any structure, by substituting the relevant radius for r_H in Eq. 7. Roughly the same value of g_{tsv} should apply to lipid compositions that do not form H_{II} phases, but which have acyl chain compositions homologous to those of the reference system. This is suggested by the behavior of PEs with identical main chain lengths (Lewis et al., 1989). In this series, the dimensions of the L_α and H_{II} phases lattices at T_H are nearly the same between members of the series. Moreover, the L_α/H_{II} transition occurs when the L_α phase bilayers thin to a certain critical thickness, and the temperature at which this occurs appears to be a function of the chain-melting temperature, T_c: T_H occurs at about the same temperature interval above T_c for the members of the series. C_0 is roughly constant at T_H for all these lipids, and the transition occurs when the curvature and interstice energies balance. Therefore, these observations imply that g_{tsv} is a function chiefly of T_c. Tate and Gruner (1989) showed that the monolayer thickness in the H_{II} phase was nearly the same across a wide temperature range in DOPE and a DOPE/DOPC mixture, despite the difference in C_0 between the two compositions. Taken together, these studies imply that g_{tsv} for lipids with the same average chain lengths and same T_c will be the same, even if the lipids have different C_0 values. This should be particularly valid for a homologous series of lipids with identical acyl chains, like DOPE, DOPE-Me (*N*-monomethylated dioleoylphosphatidylethanolamine), and DOPC. These lipids have very similar T_c: for DOPE, −16°C (Marsh, 1990); for DOPE-Me, −12.5°C (Gruner et al., 1988); and for DOPC, −19°C (Marsh, 1990). The same arguments apply to the evaluation of g_{asv} (Eq. 8).

Effects of lipid composition on intermediate energies

Keller et al. (1993) studied the structural parameters of H_{II} phases of DOPE, and mixtures of DOPE, DOPE-Me, and DOPC. In this series, C_0 appears to be a function only of the head group identity. Moreover, the net C_0 of a mixture of

these lipids is the mole fraction-weighted sum of the C_0 values of the pure components. As discussed above, the values of k_m for very different lipid compositions are fairly similar, and g_{tsv} should be the same for lipids with homologous acyl chains and similar values of T_c. Therefore, it is possible to compare the energies of intermediate structures in lipid compositions of different phase behavior within this homologous series simply by changing the value of C_0 at constant values of k_m and g_{tsv}.

INTERMEDIATE STRUCTURES AND FUSION MECHANISMS

A. Stalk Intermediates

A stalk is a semitoroidal structure that forms between two closely apposed membranes, and makes the facing monolayers of the two membranes continuous (Fig. 2 *B*). This is the same geometry proposed by Markin and others (Markin et al., 1984; Chernomordik et al., 1985, 1987; Leikin et al., 1987; Kozlov et al., 1989). The stalk is cylindrically symmetric about the vertical axis (i.e., has the same shape as a capstan or the waist of an hourglass), and is characterized by three dimensions: the marginal radius r, the axial radius R, and the marginal angle ϵ. R is equal to half the monolayer thickness, $h/2$. The angle ϵ represents the extent of deformation of the original membranes at the site of contact (Fig. 2 *B*): ϵ equals zero if the stalk forms between two planar bilayers, and ϵ is greater than zero if the stalk forms at a site where the two membranes are puckered toward each other. The stalk is assumed to form at a transient contact point of the two apposed membrane interfaces. Only a very small area of interface has to be closely apposed in order to do this, and energy-intensive processes (like rupture of the two facing monolayers) also only have to occur over this small area. The separation between lipid/water interfaces at the margin of the stalk is $2(r - h/2)\cos\epsilon$.

Markin et al. (1984) proposed that a stalk (Fig. 2 *B*) expands radially as depicted in Fig. 2 *C*. As the semitoroidal connection between the *cis* monolayers expands in radius (i.e., as R in Fig. 2 *B* increases), the *trans* monolayers dimple inwards and meet with hydrophobic sides in contact in the center of the structure (Fig. 2 *C*). Here, this structure is referred to as a *trans* monolayer contact (TMC). Markin et al. (1984) suggested that a TMC would radially expand to a much larger extent than depicted in Fig. 2 *C*. In their analysis, x would increase until an extensive single-bilayer diaphragm formed between the two original liposomes. A membrane tension resulting from unequal area deformation of the *cis* and *trans* monolayers would eventually rupture it, producing fusion.

The present analysis, done in the light of more recent data, suggests a different sequence of events following stalk formation. The present analysis differs from that of Markin at al. (1984), because it includes the effects of hydrophobic interstice energy and the curvature energy of the *trans* monolayers. The energies of the intermediates pictured in Fig. 2 were all calculated using Eqs. 2, 6, 7, and 8 as a function of

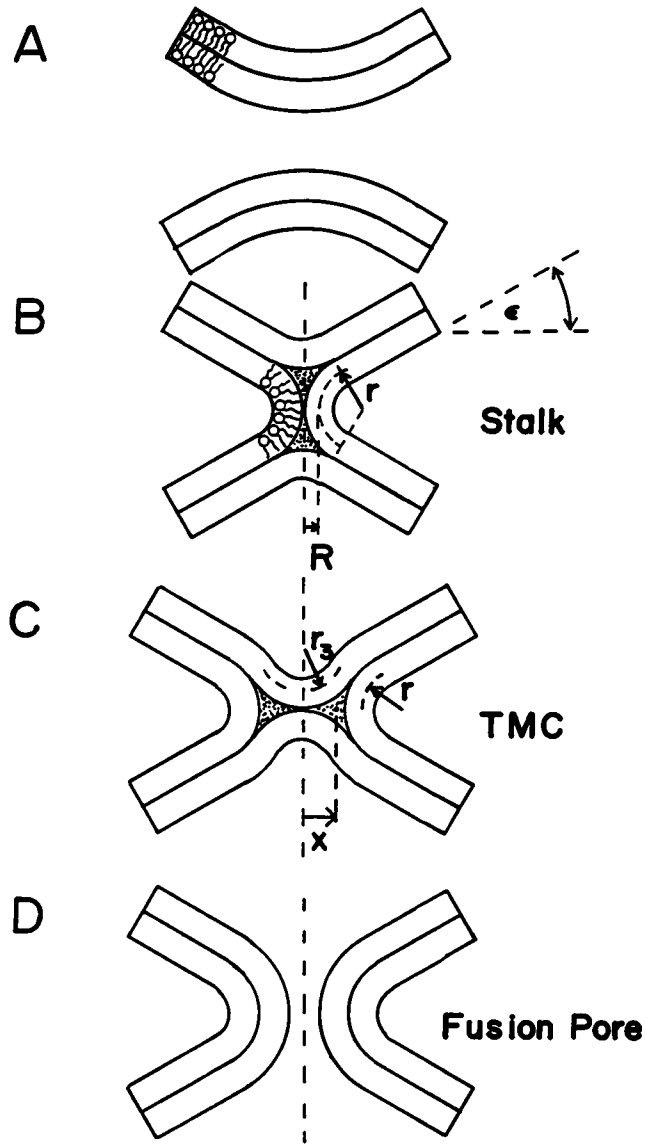

FIGURE 2 Modified stalk mechanism of membrane fusion. Two bilayers (*A*) are closely apposed. A stalk (*B*) forms following close apposition of the interfaces. The stalk is cylindrically symmetric about the dashed vertical axis. The marginal and axial radii (r and R, respectively) are evaluated at the midsurface of the lipid monolayer. The marginal angle, ϵ, is determined by the extent of deformation of the two membranes at the stalk formation site. For certain values of r and C_0 (see text), the monolayers of the stalk undergo a continuous deformation into a TMC (*C*). The TMC contains a ring-shaped locus of TSV, with centroid radius x. The dimple ruptures under curvature and interstice-generated stress to form a fusion pore (*D*) (also called an interlamellar attachment).

stalk marginal radius r and marginal angle ϵ. The explicit forms of Eq. 2 for the different geometries are given in the Appendix. The value of r_3 in Fig. 2 *C* was determined by minimizing the free energy of the TMC at each value of C_0 and representative values of r. It was found that to good accuracy one value of r_3 minimized the TMC energy for all r between 2 and 4 nm (i.e., the energy is within about 5% of the minimal value for the extreme values of r).

The tendency of the TMC to expand radially and form a planar bilayer diaphragm between the two original bilayers

was also tested. For most values of r and C_0, the TMC energy increased as the diameter of this diaphragm increased. Hence TMC should not expand into a bilayer diaphragm, and should appear as depicted in Fig. 2 *C*. For large values of r (3–4 nm) the TMC has a slight tendency to form a planar diaphragm ca. 1 nm or less in diameter. Interestingly, as systems approach the L_α/H_{II} phase transition, the TMC has a more pronounced tendency to form larger diaphragms. This has important implications for L_α/inverted phase transition mechanisms and liposome fusion in the vicinity of these transitions (D. Siegel, manuscript in preparation).

The results of intermediate energy calculations yield the following physical picture of the fusion mechanism.

(A) For many values of r, ϵ, and C_0, most of the energy of a stalk is associated with the waist (the narrow connection between the two original membranes). At the most narrow point, this waist has the same cross-section as a rod micelle, and has a large and unfavorable positive curvature. This curvature energy is not very sensitive to the C_0 of the *cis* monolayer lipid composition, since the C_0 values for all phospholipid compositions are all far from the actual curvature of this surface. The free energy associated with the two ASVs is 20–30% of the total energy. For stalks with small r ($\leq$ ca. 1.5 nm) or near-zero ϵ, the curvature energy of the neck is a smaller component of the total energy, the curvature energy of the *trans* monolayers becomes more significant, and the total energy is more sensitive to C_0.

(B) A stalk can transform into a TMC. Depending on the dimensions of the stalk, additional activation energy may be required for this. However, for a certain range of values of r and C_0, the TMC (Fig. 2 *C*) is lower in energy than the initial stalk, and TMC formation is spontaneous. No energy-intensive steps are needed to interconvert these two structures: the TMC is formed by continuous deformations of continuous monolayers. The principle factor driving TMC formation is that the curvature energy of the outer, semitoroidal monolayer of the stalk decreases rapidly as R increases. When R increases, the *trans* monolayers dimple inwards to prevent formation of a large void inside the structure. The factor opposing dimpling is the curvature energy necessary to deform the *trans* monolayers into the dimple, which depends on C_0 of the *trans* monolayer lipid composition. Forming the dimple also creates a ring-shaped locus of hydrophobic interstice (TSV) (*stippled area* in Fig. 2 *C*). x is the radius of the centroid of this interstitial volume. The interstice energy of the TMC is $2\pi x g_{tsv}$, where g_{tsv} is given by Eq. 7 and x by Eq. A3. Expansion of the TMC into a planar bilayer diaphragm increases x, and thus increases the total energy, so this expansion is disfavored. Therefore it is unlikely that fusion will proceed via formation of an extended bilayer diaphragm, followed by development of a hole in the single bilayer diaphragm, as previously proposed (Markin et al., 1984; Chernomordik et al., 1985, 1987; Leikin et al., 1987; Kozlov et al., 1989).

(C) The TMC can reduce its free energy by forming a fusion pore (Fig. 2 *D*). For all ranges of parameters considered (r = 1.5–4 nm, C_0 = +0.1 to −0.3 nm^{-1}, ϵ = 0 – 30°), the free energy of the TMC is > 200 kT higher than the free energy of the fusion pore. Most of the unfavorable curvature and interstice energy of the TMC is concentrated in the dimple. The monolayers of the dimple have a substantial positive curvature energy. Moreover, the lipid that is most stressed by the presence of the interstice is the lipid immediately adjacent to the interstice, which includes the lipids in the monolayers of the dimple. Rupture of the dimpled monolayers to form a fusion pore releases some of the curvature energy and all of the interstice energy. It can be shown that each lipid molecule in the dimple is stressed by 2–5 kT compared to lipid in the monolayer lining the fusion pore, depending on C_0. Rupture of the single-bilayer dimple is a highly localized event, requiring energy-intensive processes acting only on a few lipid molecules.

The stalk mechanism described here is significantly different from earlier models. Interstice energy plays an important role: it keeps the TMC from expanding into a bilayer diaphragm. This concentrates the curvature and interstice stresses within the dimple, which drives fusion pore formation.

B. Inverted micellar intermediates

The IMI-mediated fusion mechanism (Siegel, 1986b) is shown in Fig. 3. The IMI (Fig. 3 *B*) is cylindrically symmetric about the vertical axis and consists of a spherical inverted micelle inside a semitoroidal outer monolayer (e.g., a soccer ball nestled inside an automobile tire rim). In order for an IMI to form between two bilayers, the interfaces have to be closely apposed, and the lipid/water interfaces ruptured, on a circular locus about $2r$ (ca. 6 nm) in diameter. An IMI forms a fusion pore (also called an interlamellar attachment or ILA (Siegel, 1986a, 1986b)) via coordinated rupture of the two pairs of monolayers at the axis of the structure at the top and bottom of the inverted micelle. Note that energy intensive processes have to act on larger numbers of lipids to form IMIs and ILAs than to form stalks and TMCs.

The IMI contains two large-diameter rings of TSV, which makes the structure relatively unstable. The regions of *trans* monolayers overlying these TSVs form ring-shaped depressions to lower the volume of the interstices. It was assumed that the negative radius of curvature of these depressions is the same as the marginal radius r. The IMI energy is minimal when the radius of the inverted micelle equals the marginal radius. IMIs can form between membranes that are deformed as in Fig. 2 *A*: this deformation is characterized by a marginal angle ϵ, just as with stalks (Fig. 2 *B*). Fig. 3 is drawn with ϵ = 0. As with stalks, the IMI energy decreases with increasing ϵ.

NUMERICAL RESULTS

Stalk energy

The free energy of stalk intermediates relative to an equivalent area of planar bilayer is plotted in Fig. 4 as a function

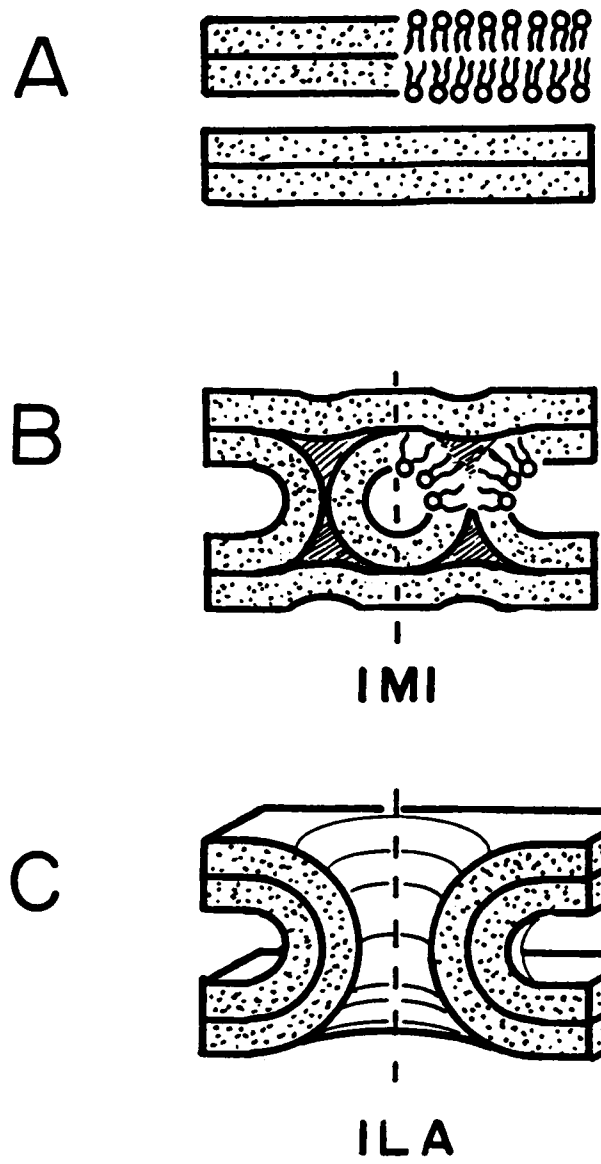

FIGURE 3 Mechanism of fusion via IMI formation. Two apposed membranes (*A*) form an IMI (*B*) after close apposition of the interfaces. The IMI is cylindrically symmetric about the dashed vertical axis, and consists of a spherical inverted micelle inside a semitoroidal outer monolayer. It contains two rings of TSV (above and below the inverted micelle, respectively), which are depicted in cross-section as cross-hatched areas. For certain values of C_0, the IMI can transform into an ILA (*C*), fusing the two original membranes.

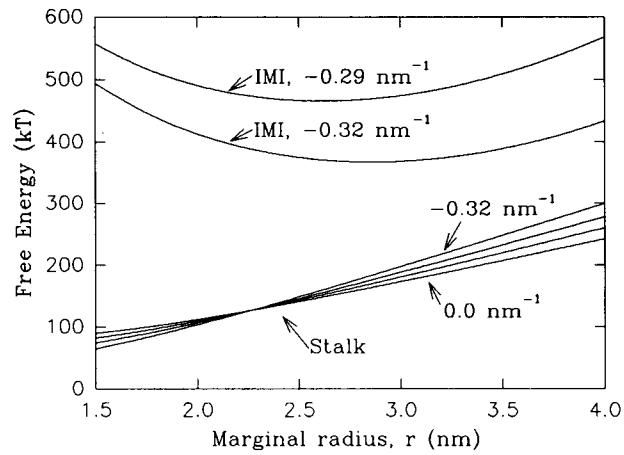

FIGURE 4 The free energies of stalks (*lower curves*) and IMIs (*upper curves*) relative to equivalent areas of planar bilayer, plotted as a function of marginal radius r for different values of the spontaneous curvature, C_0, of the lipid composition, with $\epsilon = 30°$, for both stalks and IMIs. Energy is in units of kT at 25°C, where k is Boltzmann's constant. Stalks: the The four curves given above were calculated for (from top to bottom at the right-hand side of the figure) $C_0 = -0.323, -0.2, -0.1$, and 0 nm^{-1}; respectively. IMIs: The two cases above are calculated for $C_0 = -0.323$ and -0.286 nm^{-1}, corresponding roughly to DOPE at T_H and ca. 10° below T_H, respectively.

of marginal radius r, for several representative values of C_0 (lower set of lines). The value of ϵ is 30°, but the curves have the same shape and ordering with respect to C_0 for ϵ values down to 0°. The energy increases as ϵ is decreased to zero (which corresponds to stalk formation between apposed planar bilayers), particularly for large values of r.

We do not have an a priori way to determine what value of r a stalk or IMI should have in given circumstances, so the energies of these intermediates are calculated as a function of r across the range of relevant values. The plots of intermediate energy vs. r are of very similar form for all values of C_0, so the effects of changes in lipid composition can be assessed without having to assume a value for r. The 4 nm upper limit to r is fairly arbitrary: stalk energies increase monotonically with r, and stalks much larger than this will be very unstable. The lower limit of 1.5 nm was chosen since the radii in TMCs and fusion pores forming from stalks with smaller r would be ca. 1 nm or less (water pores only a couple of angstroms in diameter). Under those conditions, the simple geometries assumed for TMCs and fusion pores would be unrealistic, and additional assumptions would have to be made. Moreover, the curvature energy equations may be inapplicable at such small radii.

Two features of the stalk energy are obvious in Fig. 4. First, the energy of a stalk increases with increasing r. Second, for $\epsilon = 0$ to 30 degrees and this range of r, the stalk energy is fairly insensitive to C_0 of the lipid composition, for the range of C_0 relevant to pure phospholipids. In Fig. 4, C_0 varies between values for lipids which are very stable in the L_α phase ($C_0 = 0$) to lipids at the L_α/H_{II} transition temperature (e.g., $C_0 = -0.32$ nm^{-1} for DOPE (Rand et al., 1990)). Even at the largest and smallest values of r, the stalk energy changes by only 25% between extremes of C_0.

Comparison of stalk and IMI energies

The free energy of an IMI compared to an equivalent area of planar bilayer is also plotted in Fig. 4 (*upper pair of lines*) for two values of C_0; −0.32 and −0.29 nm^{-1}. These values correspond to pure DOPE at temperatures of T_H and ca. 10 K below T_H, respectively (Rand et al., 1990; Gruner et al., 1988). It is obvious that the IMI energy is considerably larger than the energy of a stalk at all values of r. Moreover, the IMI energy increases rapidly with increasing C_0, as is shown by

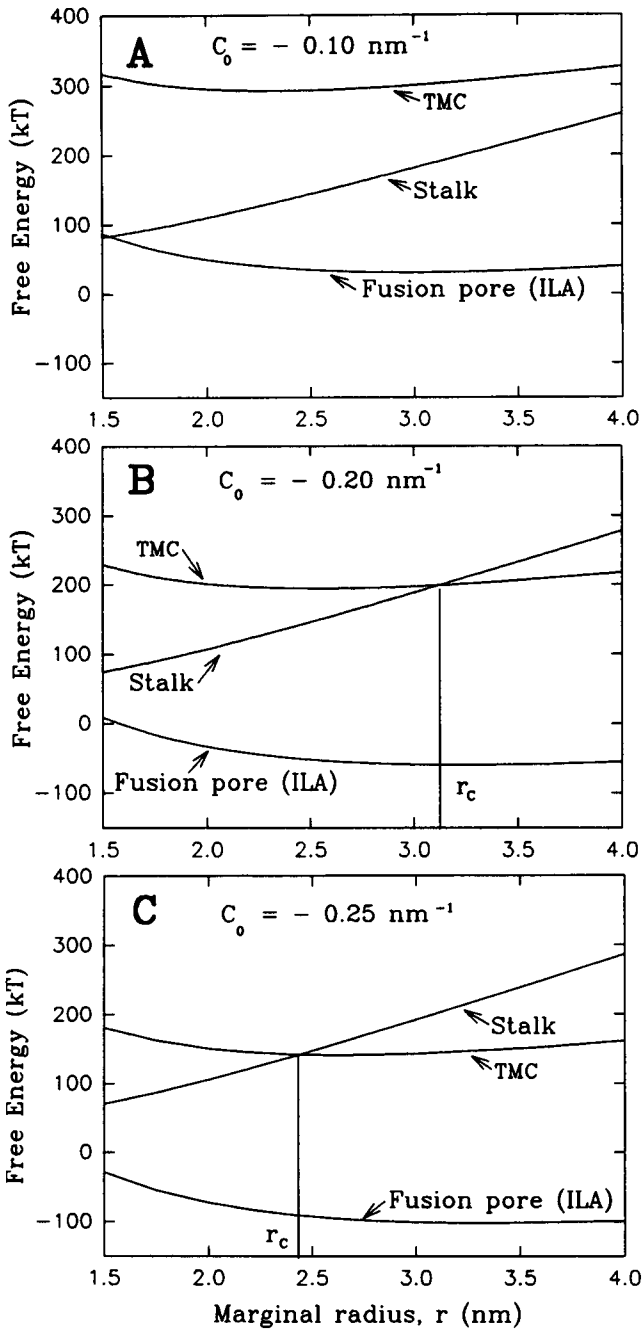

FIGURE 5 The free energies of stalks, TMCs, and fusion pores plotted as a function of r for different values of C_0, with $\epsilon = 30°$. (*A*) $C_0 = -0.1$ nm^{-1}, corresponding roughly to pure DOPC. TMC formation, and fusion, should be rare. (*B*) $C_0 = -0.2$ nm^{-1}, corresponding to a roughly equimolar DOPC/DOPE mixture. The TMC energy is lower than in (*A*) for all values of r. Also, for $r \geq r_c$, stalks can transform spontaneously into TMCs. Fusion should occur at a much higher rate than in (*A*). (*C*) $C_0 = -0.25$ nm^{-1}, corresponding to a DOPE-rich DOPC/DOPE mixture. The TMC energy is lower than in (*A*) and (*B*). Also, the value of r_c, and the energy of stalks with r = r_c, are both lower than in (*B*). Fusion should occur at an even higher rate.

the large difference in energy between the IMI curves for $C_0 = -0.32$ and -0.29 nm^{-1}. The value of ϵ is 30° for both stalks and IMIs in Fig. 4, but the energies are in the same relationship for the stalks and IMIs at any value of ϵ down to 0°. These results indicate that stalks are lower-energy structures than IMIs, even for systems at T_H.

Relative energies of stalks, TMCs, and fusion pores

The free energies of stalks, TMCs, and fusion pores are plotted as a function of r for three different values of C_0 and $\epsilon = 30°$ in Fig. 5. The C_0 values in Fig. 5 of −0.1, −0.2, and −0.25 nm^{-1} correspond roughly to pure DOPC, a DOPC-rich DOPE/DOPE mixture, and a DOPE-rich DOPE/DOPC mixture, all at 25°C, respectively. The free energy of the TMC decreases at all values of r as C_0 decreases. Since a TMC must form in order for fusion to occur (Fig. 2), this shows that the activation energy for fusion decreases as C_0 decreases. This is emphasized in Fig. 6, where the minimum energy needed to form a TMC is given as a function of C_0 of the lipid composition for $\epsilon = 30°$. This energy corresponds to the minimum free energy of activation required for fusion in systems with the specified C_0.

In Fig. 5, note that as C_0 decreases the energy of the TMC dips below the stalk energy for values of r above a certain value, r_c, at each C_0 (Figs. 5 *B* and 5 *C* versus 5 *A*). This is significant because a stalk can generally reduce its energy by shrinking (decreasing the value of r). However, in order for fusion to occur, the stalk must first form a TMC (Fig. 2). Whether or not the stalk shrinks or forms a TMC is probably determined by the relative rates of the two processes. When $r \geq r_c$, TMC formation is spontaneous, which presumably makes fusion more likely. The energy needed to form a stalk of $r = r_c$ decreases with decreasing C_0 (Figs. 5 *B* and 5 *C*). This is a second reason why fusion should be more facile at lower values of C_0.

The results in Fig. 5 show that while fusion should be rare in pure DOPC systems (Fig. 5 *A*), fusion should occur more

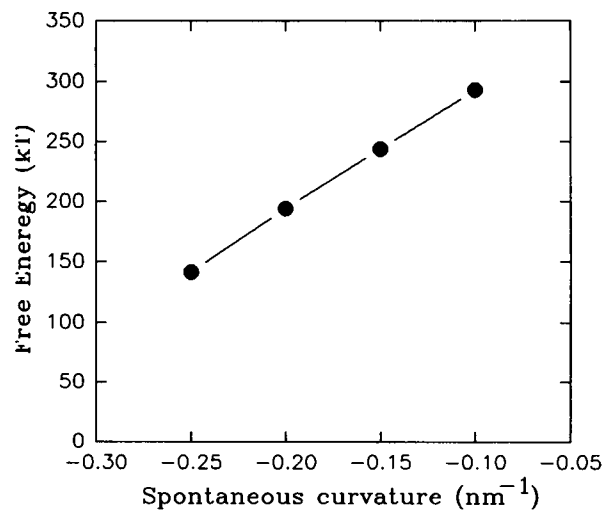

FIGURE 6 Plot of the minimum energy necessary to form a TMC as a function of the spontaneous curvature, C_0, of the lipid composition, with $\epsilon = 30°$. For each value of C_0, the minimum value of the TMC energy as a function of r was calculated. This energy is the minimum total activation energy required for fusion at the given value of C_0.

frequently as the mol fraction of DOPE is increased, or as the temperature of the system is increased towards T_H so as to decrease C_0 (Figs. 5 *B* and 5 *C*). Note also that the fusion pores become thermodynamically stable with respect to planar bilayers below a certain C_0 value, which has important implications for nonbilayer phase stability (D. Siegel, manuscript in preparation).

Effect of *trans* monolayer lipid composition

Fusion produces a single continuous bilayer from two apposed bilayers, so it is expected that the composition of *both* the outer (apposed, "*cis*") monolayers and the inner (nonapposed, "*trans*") monolayers affects the rate of the fusion process. Results calculated for symmetric and symmetric lipid compositions are show in Fig. 7. Results for bilayers with a symmetric lipid composition are shown in Fig. 7 *A*, where C_0 is -0.1 nm^{-1} (corresponding roughly to pure DOPC at room temperature). Fusion via a stalk mechanism should be rarely observed in this composition, because the energy of the TMC is always higher than the energy of the stalk. Decreasing C_0 of only the *trans* monolayers to -0.25 nm^{-1} (Fig. 7 *B*), which corresponds roughly to a DOPE-rich DOPE/DOPC mixture at room temperature, lowers the TMC energy and makes fusion occur more easily. Similarly, if the *trans* monolayer lipid composition retains a C_0 of -0.1 nm^{-1} but the *cis* monolayer C_0 is reduced to -0.25 nm^{-1} (Fig. 7 *C*), fusion also occurs more readily compared to the symmetric case (Fig. 7 *A*). Decreases in the *trans* monolayer C_0 reduce the energy necessary to form the dimple in the TMC, while decreases in *cis* monolayer C_0 stabilize the semitoroidal monolayer of both the stalk and TMC.

More subtle effects of bilayer asymmetry would be expected when the lipid in the bilayers is very close to T_H. Under these circumstances, stalks may form H_{II} phase precursors, and any TMCs that form should have a tendency to radially expand, decreasing the driving force for fusion pore formation (D. Siegel, manuscript in preparation).

Effects of positive values of C_0

The value of C_0 of a lipid composition can become positive upon addition of certain single-chain surfactants (e.g., addition of low levels of lysolipids to DOPC). The energies of stalks, TMCs, and fusion pores are plotted in Fig. 7 *D* for a case in which C_0 is $+0.1$ nm^{-1} for the *cis* monolayer lipid

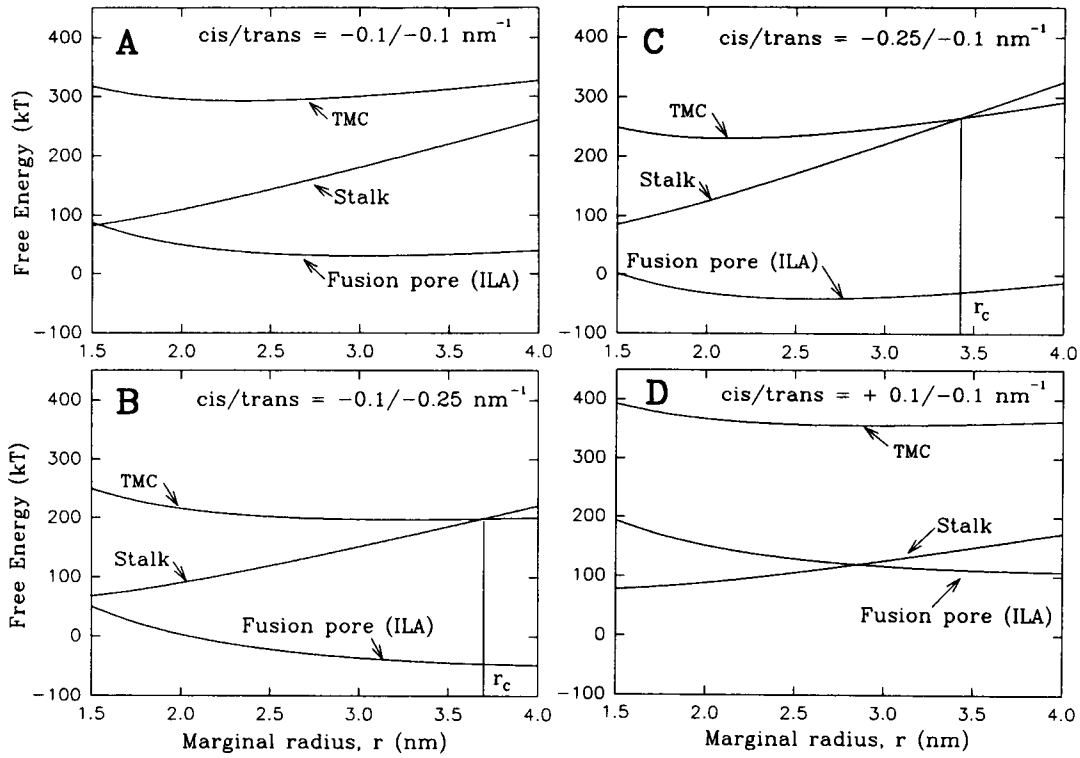

FIGURE 7 Effect of transbilayer asymmetry and positive C_0 on the energies of intermediates in the modified stalk mechanism. (*A*)Symmetric bilayers, where C_0 for the lipid in each monolayer is -0.1 nm^{-1} (corresponding roughly to pure DOPC). Fusion events should be rare. (*B*) Asymmetric bilayers in which C_0 of the *cis* (apposed) monolayers is still -0.1 nm^{-1} (e.g., DOPC), but C_0 for the *trans* (nonapposed) monolayers is -0.25 nm^{-1} (e.g., DOPE-rich DOPE/DOPC mixture). Fusion should be much more facile than in A, above, since the TMC energy is lower and TMCs form spontaneously for $r \geq r_c$. This case corresponds to fusion of right side-out biomembranes (e.g., viral infection of cells). (*C*) Bilayers with the reverse asymmetry of those in *B*; *cis* $C_0 = -0.25$ nm^{-1}, *trans* $C_0 = -0.1$ nm^{-1}. Fusion should also be much more facile than in case *A*. This case corresponds to fusion of intracellular membranes (e.g., exocytosis). (*D*) Asymmetric bilayers with *cis* monolayer $C_0 = +0.1$ nm^{-1} (expected for membranes were equilibrated with sublytic concentrations of detergents). The stalk energy is much lower than in (*A*), but the TMC and fusion pore energies are much higher. Aqueous contents mixing should be rare.

and -0.1 nm^{-1} for the *trans* monolayer lipid, with $\epsilon = 30°$. This situation models a dispersion of DOPC liposomes exposed to a sublytic concentration of a surfactant like lysolecithin, which would make C_0 of the *cis* monolayers positive. Comparison with Fig. 7 *A* shows that making the *cis* monolayer C_0 positive increases the energy of the TMC and the fusion pore. This is expected because the net curvatures of the TMC and fusion pore are negative, and the curvature energies of TMCs and fusion pores are thus adversely affected by a positive C_0. The energies of TMCs and fusion pores always increase when C_0 is made positive, for all choices of r and ϵ. The net effect of this change should be to decrease the rate of fusion as assayed by aqueous contents mixing. If C_0 of both monolayers is positive, this effect is even more pronounced.

The effect of positive C_0 values on the energy of stalks is more complicated, and depends on the value of r and ϵ of the stalk. Stalks with $\epsilon \approx 30°$ (plotted in Fig. 7 *D*) have positive average curvatures for all relevant r values, but stalks with near-zero values of ϵ and small values of r have negative average curvatures. Positive C_0 values slightly *decrease* the energy of stalks with large values of ϵ, and slightly *increase* the energy of stalks with $\epsilon = 0$. Thus, changing C_0 of a system to positive values may either increase or decrease the stalk formation rate. However, the energy required to form TMCs determines the fusion rate: a stalk can only produce fusion via formation of a TMC (Fig. 2). A given change in C_0 from a negative to a positive value affects the TMC energy much more than the stalk energy under all circumstances (e.g., ca. 150 kT or more versus ca. 40 kT, respectively, for $r = 1.5$ nm, $\epsilon = 0°$ and a change in C_0 from -0.1 nm^{-1} to $+0.1$ nm^{-1}). Therefore, increasing C_0 to positive values should decrease fusion rates.

DISCUSSION

This work describes a method for estimating the free energy of intermediates in membrane fusion in different lipid compositions. The estimated energies can be used to qualitatively compare different hypothetical fusion mechanisms, and to decide which best fits the observed behavior. In particular, testable (although qualitative) predictions about the effects of lipid composition and bilayer composition asymmetry on fusion rates can be made.

Two general conclusions arise from calculations of intermediate energies in stalk and IMI fusion mechanisms. The first is that interstice energies can be a substantial contribution to the total energy. This contribution has not been explicitly considered previously in fusion intermediate modeling, and should change our conceptions of fusion mechanisms. For instance, consideration of interstice energies makes it necessary to modify the stalk mechanism as originally proposed (Markin et al., 1984). Moreover, interstice effects are almost certainly important in fusion mechanisms in general. Because of the poor coupling between monolayers of each bilayer, most proposed fusion mechanisms require formation of a structure that involves only the *cis* monolayers of the two bilayers, followed by a step that ruptures the *trans* monolayers. If the first step involves formation of continuous monolayer structures between the two membranes, hydrophobic interstices must form within each bilayer where the leaflets separate. Addition of long-chain alkanes reduces the interstice energy in H_{II} phases, which results in a drastic reduction in T_H (Kirk and Gruner, 1985; Tate and Gruner, 1987; Sjölund et al., 1987; Siegel et al., 1989b). Similarly, we should expect the inclusion of low levels of long-chain alkanes in lipid bilayers to substantially affect observed fusion and lipid mixing behavior. For example, addition of low levels (several mol%) of hexadecane to the lipids would stabilize both stalks and TMCs, increasing the fusion rate. Higher levels should do the same, but might also reduce the driving force for TMC rupture and fusion. Low levels of hexadecane have already been observed to substantially increase the rate of divalent cation-induced lipid mixing between phosphatidylserine membranes (A. Walter, P. L. Yeagle, and D. P. Siegel, manuscript submitted). In a preliminary report of the theoretical methods discussed in the present paper, the contributions of interstice energies were overestimated (Siegel, 1993).

The second general conclusion is that the modified stalk mechanism (Fig. 2) is a more likely mechanism for fusion in a wider range of lipid compositions than the IMI mechanism (Fig. 3). The energies of the intermediates in the modified stalk mechanism are lower in all cases. Moreover, the intermediates in the modified stalk mechanism can be created and interconverted by action of energy-intensive processes (e.g., monolayer rupture) over smaller areas than in the IMI mechanism. These two considerations suggest that the activation energies are lower in the modified stalk mechanism, and that the corresponding rates are much faster. This is true even for systems at T_H, where IMIs should form most readily (Siegel, 1986a,b). This result has important implications for models of the of L_α/H_{II} phase transition mechanism (D.Siegel, manuscript in preparation). The comparison of stalk and IMI energies in previous work (Siegel, 1986a) was made on the basis of cruder estimates of intermediate energies, and is incorrect in light of the present results.

Intermediate energies and fusion rates

The intermediate energies calculated by the present method can only be used to make qualitative comparisons between fusion rates expected for different mechanisms or in different lipid systems. The intermediate energies are lower bounds to the true activation energy needed to form the intermediate. The "cost" of the energy-intensive processes involved (e.g., rupture of the monolayers, etc.) has to be included, and the modes of motion have to be known, in order to calculate rate constants. We do not have sufficiently detailed (molecular level) knowledge of the mechanism to calculate those contributions. The mechanisms considered here also require multiple steps in rapid succession (e.g., Fig. 2), and the ob.

served overall fusion rate is not easy to interpret in terms of the rates of intermediate steps (Bentz, 1992). Finally, the individual steps are likely to be cooperative processes that are not based on a single molecular mode of motion, so the energies calculated for each step do *not* correspond to the "activation energies" obtained from Arrhenius plots of fusion rates. Hence the temperature dependence of observed fusion rates does not yield values for these activation energies. Note also that the energies estimated here are free energies, while the Arrhenius activation energy is an enthalpy (e.g., Castellan, 1971).

Two caveats should be borne in mind when comparing predictions made on the basis of intermediate energies with observed fusion behavior. First, liposome fusion is a multistep process; liposome aggregation followed by fusion. Often, only the overall rate is reported. The predictions made here based on intermediate energies refer only to the rate of the steps subsequent to close apposition of the interfaces. To observe differences in this rate, the overall rate must be measured in a concentration regime where the rate of liposome aggregation is not the major influence on the overall rate (Bentz et al., 1983).

The second caveat is that the fusion rate referred to here is the rate of mixing of aqueous contents. Many authors measure the rate of "fusion" by measuring the rate of contact-induced lipid mixing between liposomes (for a review of the assay methods, see Düzgünes and Bentz (1988)). It is obvious from Figs. 2 and 3 that lipid mixing assays can report the rate of processes that are not fusion. For instance, in some systems stalks and even TMCs might form, but revert to the original separated bilayer structures. In addition, at T_H the stalks probably mediate rearrangement of the bilayers into H_{II} phase (D. Siegel, manuscript in preparation), releasing the contents of the original liposomes. Both of these processes would mix the lipids of the two original bilayers at least to some extent, but neither process results in fusion with retention of aqueous contents of the original liposomes. The extent of lipid mixing via transient stalks or TMCs in the absence of fusion pore formation is uncertain because we do not know the lifetimes of these structures. A recent time-resolved cryoelectron microscopy study of the L_α/H_{II} transition (D. Siegel et al., submitted for publication) indicates that intermediates like stalks may have half-lives shorter than 1 ms. It can be shown that stalks with a lifetime of 0.1 ms would mediate the exchange of only ca. 1% of the lipids in two 0.1-μm-diameter liposomes.

Fusion behavior of the modified stalk mechanism as a function of C_0

In general, the rate of fusion is expected to increase with decreasing C_0 (Fig. 6), primarily on account of effects of C_0 on the energy of TMCs. Lipid mixing rates between apposed bilayers should generally follow the same trend. However, lipid mixing and contents mixing via a modified stalk mechanism can proceed at substantially different rates in two sorts of systems. First, in some systems, stalks may form transiently but not form TMCs and fusion pores. An example is shown in Fig. 5 *A* ($C_0 \approx -0.1$ nm^{-1}, corresponding roughly to DOPC at room temperature): TMCs have much higher energies than stalks in this system. This should result in some lipid mixing via stalks, but no (or rare) contents mixing. As noted above, the extent of lipid mixing via stalks may be negligible. Second, for C_0 smaller than ca. -0.25 nm^{-1}, the contents-mixing rate may plateau and even decrease as C_0 decreases to a value corresponding to formation of H_{II} phase, while the lipid mixing should monotonically increase. This is because the TMC exhibits three tendencies as systems approach T_H (D. Siegel, manuscript in preparation): it tends to radially expand; r_3 (Fig. 2 *C*) increases; and the curvature energy of the *trans* monolayer dimple decreases. All these trends stabilize the TMC and reduce the driving force for fusion pore formation. However, the expanded TMC would make a large, comparatively stable lipid connection between apposed bilayers, which would promote extensive lipid mixing.

Observed effects of C_0 on fusion rates

The C_0 dependence of overall fusion rates has been studied in a number of systems, including PEs, PE analogs, and PE/PC and PE/PS mixtures. In these studies, C_0 was altered by changing the amount of PE in the lipid composition. However, the rate measurements have nearly all been done under aggregation rate-limited conditions. This is unfortunate, because changes in the mol fraction of (noncharged) PE also change the strength of repulsive electrostatic and hydration forces between bilayers. Therefore it is not clear if the primary effect of PE was on the rate of the aggregation or fusion step. Stopped-flow techniques make it possible to measure overall fusion rates in the proper kinetic regime to separate these effects (e.g., Walter and Siegel, 1993). Because of the scarcity of measurements in the proper kinetic regime, little is known about the C_0 dependence of the rate of the fusion step per se.

With those caveats, however, the overall fusion rate dependence in many systems is as expected on the basis of a modified stalk mechanism. In mixtures of PE and PS, addition of PE increases the fusion rate and decreases the concentration of divalent cations necessary to trigger liposome fusion (Düzgünes et al., 1981, 1984; Silvius and Gagné, 1984; Stamatatos and Silvius, 1987). In PE or PE-analog containing systems, overall lipid mixing and aqueous contents-mixing rates are also as expected for a stalk-mediated mechanism (Bentz et al., 1985, 1987; Ellens et al., 1986a, b, 1989; Brown and Silvius, 1989; Siegel et al., 1989a). Both rates increase as C_0 decreases (i.e., as either temperature or the PE content increases), although contents mixing is not observed in all cases (Bentz et al., 1985). The contents-mixing rate often increases with temperature and goes through a maximum at $T \approx T_H$ (Ellens et al., 1986a, b, 1989; Siegel et al., 1989a), decreasing thereafter, while the lipid mixing rate increases monotonically. This behavior is compatible with stalk-mediated interactions near T_H, since

TMCs should expand radially (i.e., form fewer fusion pores) under those conditions. Brown and Silvius (1989) showed that if the PE in a lipid mixture is replaced by a PE analog with a modified head group, the fusion rate at a constant temperature is inversely correlated with T_H of the analog. C_0 decreases as the temperature increases towards T_H (Tate et al., 1991; Gruner et al., 1988). Thus, the results of Brown and Silvius (1989) also show that the fusion rate increases with decreasing C_0, as expected for a modified stalk mechanism.

In addition to requiring a larger activation energy in general, an IMI-based mechanism is not as consistent with the observed temperature dependence of fusion near T_H. As discussed by Ellens et al. (1989), an IMI-based fusion mechanism cannot readily explain the observation of fusion at temperatures as much as 35K below T_H. As shown in Fig. 4, IMI energies increase rapidly as C_0 is increased (or as T decreases below T_H), so that IMI-mediated fusion should shut off at temperatures not far below T_H. In contrast, the energy needed to form a fusion-capable TMC is less sensitive to changes in C_0 (less sensitive to T near T_H), and a modified stalk mechanism better explains the observed temperature dependence.

Effects of transbilayer asymmetry

The *trans* monolayer C_0 has a substantial effect on the energy of TMCs. Hence, the C_0 of the *trans* monolayer lipid should substantially affect the aqueous contents and lipid mixing behavior of a system. Generally, decreasing C_0 of the *trans* monolayer should facilitate both contents and lipid mixing. As noted above, more subtle effects may occur when C_0 of both *cis* and *trans* monolayers are such that each lipid composition is near its value of T_H.

Studies of the effects of transbilayer asymmetry on model membrane fusion are starting to appear (Bentz et al., 1987; Wilschut et al., 1992; Eastman et al., 1992). Unfortunately, so far these studies give us little information about the effects of transmembrane gradients in C_0. In the experiments of Eastman et al. and Wilschut et al., membrane asymmetry was established by changing the transbilayer distribution of a minor charged component with a pH gradient. The effects of the redistribution on C_0 of each monolayer were not determined. Moreover, the present theory does not take electrostatic effects into account, which are certainly critical in the divalent cation-induced fusion process occurring in the systems investigated by Eastman et al. and Wilschut et al.

In vivo, biomembrane lipid asymmetry probably has many functions. One function may be modulation of cellular membrane fusion activity. It may be significant that the lipid bilayer asymmetry found in vivo is optimal for fusion with retention of membrane stability via a modified stalk mechanism. For symmetric bilayers, fusion should occur most readily via this mechanism for C_0 values less than ca. -0.25 nm^{-1} (Fig. 6). However, these C_0 values correspond to systems close to T_H, and symmetric membranes are unstable when apposed close to T_H: liposomes often undergo extensive leakage upon aggregation under those circumstances (Bentz, 1985, 1987; Ellens et al., 1986a, b, 1989; Siegel et al., 1989a). This leakage is probably due to the formation of H_{II} phase or H_{II} precursors. Leakage is obviously incompatible with the requirement for nonleaky fusion and stable membranes in vivo. In contrast, Fig. 7, *B* and *C*, indicates that asymmetric bilayers form fusion-capable TMCs with energies nearly as low as in symmetric bilayers with low C_0. These asymmetric membranes are stable in the L_α phase, yet should fuse readily via modified stalk mechanism, yielding efficient nonleaky fusion. Biomembrane lipid compositions display the asymmetry in Fig. 7, *B* and *C*, with one leaflet enriched in inverted phase-forming lipids like PE and the other enriched in lipids like PC that only form lamellar phases (for a review, see Devaux (1991)). Fig. 7 *C* corresponds to the asymmetry encountered in processes like exocytosis. Fig. 7 *B* corresponds to fusion of right-side-out plasma membrane vesicles, as in viral infection.

Effects of positive values of C_0

Positive values of C_0 may occur in phospholipids containing small mol fractions of amphiphiles that form normal micelles (e.g., lysolecithin). As discussed in conjunction with Fig. 7 *D*, the presence of agents like lysolecithin can either increase or reduce the energy necessary to create a stalk, depending on the stalk size and the value of ϵ. However, lysolecithin should always increase the energy of TMCs. Lysolecithin can change the rate of lipid mixing via transient stalks (the extent of this lipid mixing may be negligible), and should substantially decrease the rate of TMC formation and fusion. Therefore, it is particularly interesting that Chernomordik et al. (1993) have found that lysolecithin, when administered at low (sublytic) concentrations, inhibits membrane fusion in a wide variety of biological systems. These include sea urchin cortical granule exocytosis, viral protein-mediated cell-cell fusion, patch-clamped mast cell exocytosis, and microsome-microsome fusion, all in a dose-dependent fashion. As noted above, these observations are compatible with a stalk-mediated fusion mechanism, although other explanations are possible.

The results of Lentz et al. (1992) may also be consistent with a stalk-mediated fusion mechanism. These workers found that polyethylene glycol (PEG) induces lipid mixing, but not contents mixing, between large unilamellar PC liposomes. However, more lipid mixing and some contents mixing were observed at a given PEG concentration when small molar fractions of amphipaths that form normal micelles (and presumably induce positive C_0 in bilayers) were present. These included 0.5 lipid mol% lyso-PC or palmitic acid, or 5 mol% platelet activating factor. The high concentrations of PEG (up to 40% w/w) used in these studies severely dehydrate and closely appose bilayers, which should encourage the formation of stalks with small r and values of ϵ close to 0°. Under these conditions, addition of surfactants like lyso-PC should decrease the activa-

tion energy for stalk formation, which would increase the rate of lipid mixing. In some fraction of cases the stalks may be able to produce a fusion-capable TMC structure. The results in Fig. 7 *A* imply that, in excess water, PC membranes should not exhibit much aqueous contents mixing via a modified stalk-mediated mechanism. However, high concentrations of PEG may perturb the structure of bilayer interfaces, and affect the rate of fusogenic structure formation. Lentz et al. (1992) interpreted their results in a similar fashion, but did not invoke a specific intermediate structure.

Chernomordik et al. (1985, 1987) suggested that lysolecithin could affect the fusion of bilayers in a different way. In their view, stalk formation results in formation of an extenisve single bilayer diaphragm between the two originally apposed membranes, and lysolecithin induces the formation of a pore within this single-bilayer diaphragm. The present work suggests that such diaphragms do not form: a TMC should not radially expand into a diaphragm before rupture (Fig. 2 *C*). However, it is conceivable that lysolecithin could affect the rate of TMC rupture in some fashion that is not associated with its effect on the curvature energy of the TMC or fusion pore.

How can proteins catalyze membrane fusion?

Analysis of fusion intermediates by the methods described here suggests several modes by which proteins could catalyze the formation of fusion intermediates. First, the present analysis suggests that stalks are the lowest-energy intermediate that can form between two membranes that is capable of initiating fusion. It is possible that a stalk-like structure may be an intermediate in some protein-catalyzed fusion mechanisms. Second, proteins would substantially lower the curvature energy of catenoidal or semitoroidal intermediates (e.g., stalks, IMIs) if they locally deformed the two original bilayers toward each other at the fusion site ($\epsilon > 0$, Fig. 2, *A* and *B*). This type of deformation has been observed as a prefusion step in influenza virus (Ruigrok et al., 1992). Third, stalk formation could be catalyzed by transient production of positive-C_0 patches of lipid interface. Fusion-catalyzing proteins could do this through binding of amphipathic moieties (e.g., α helical peptides) to the lipid-water interface. This tends to disrupt interactions between lipid molecules in the same interface, could promote the local deformation necessary for stalk formation, and could stabilize the positive-curvature interface of a nascent stalk. (Stalks with a wide range of r and ϵ values would be stabilized by positive C_0 values.) Fourth, proteins could lower the activation energy for fusion by stabilizing hydrophobic interstices of fusion intermediates. This might be accomplished by hydrophobic residues like isoleucine on transmembrane regions of proteins immediately adjacent to the fusion site. A similar suggestion was made previously by Gruner (1985). Alternatively, the fusion-catalyzing proteins could form a protein-lipid complex in which the base of an intermediate (e.g., the stalk) is composed mostly of proteins (Guy et al., 1992), eliminating the hydrophobic interstice. An example of a mechanism for the hemagglutinin of the influenza virus incorporating some of these elements has been suggested elsewhere (Siegel, 1993).

CONCLUSION

Analysis of the energy of hypothetical intermediates in membrane fusion can help us identify likely fusion mechanisms and generate testable predictions concerning those fusion mechanisms, for both pure lipid and protein-catalyzed membrane fusion. Although further work needs to be done to experimentally determine the C_0 dependence of the post-aggregation fusion process modeled here, the calculations show that a modified stalk mechanism is compatible with the observed fusion behavior of systems with a wide range of C_0 systems, while an IMI-mediated mechanism is not. The analysis predicts that traces of long-chain alkanes should facilitate fusion in general and also makes some predictions concerning the effects of *trans* (nonapposed) monolayer lipid composition on fusion rates via a modified stalk mechanism. These aspects of the model should be susceptible to testing through use of stopped-flow fluorescence assays (e.g., Walter and Siegel, 1993).

APPENDIX

The monolayers of the intermediates are assumed to lie on surfaces that are either segments of spheres or of toroids formed by the revolution of circles. The integrated form of Eq. 2 for each geometry is given below. Expressions were derived using the same relation between the two principal radii of curvature as used by Markin et al. (1984). Refer to Fig. 8 for definition of the dimensional variables in each case.

Toroids

Refer to Fig. 8 *A*. Note that the expressions are different when the head groups line the inside of the toroidal surface (head groups close to the axis) versus the outside of the surface.

$$G_c = \frac{2\pi k_m (R + r)^2}{r\sqrt{R^2 + 2rR}} \{\tan^{-1}[X \tan(\theta_2)] - \tan^{-1}[X \tan(\theta_1)]\}$$
$$+ 4\pi k_m (1/r \pm C_0)[(R + r)(\theta_2 - \theta_1) - r(\sin\theta_2 - \sin\theta_1)]$$
$$- 2\pi k_m (1 + R/r)(2 \pm rC_0)(\theta_2 - \theta_1), \quad \text{(A1)}$$

where $X = [(R + 2r)/R]^{1/2}$.

For monolayers on which the head groups lie outside the toroidal surface, use the upper signs in the second and third terms on the RHS of Eq.A1. For head groups on the inside, use the lower signs. Eq. A1 is valid only for $0 \leq \theta \leq \pi/2$, and gives the energy of a surface lying on only one side of the horizontal (x, y) plane. θ_1 and θ_2 are the lower and upper limits of θ, respectively.

Margins of the *trans* monolayer depression overlying the stalk

The *trans* monolayers above and below a stalk form a depression. The center is a spherical cap of radius r. The margin, indicated in Fig. 8 *B*, has a different

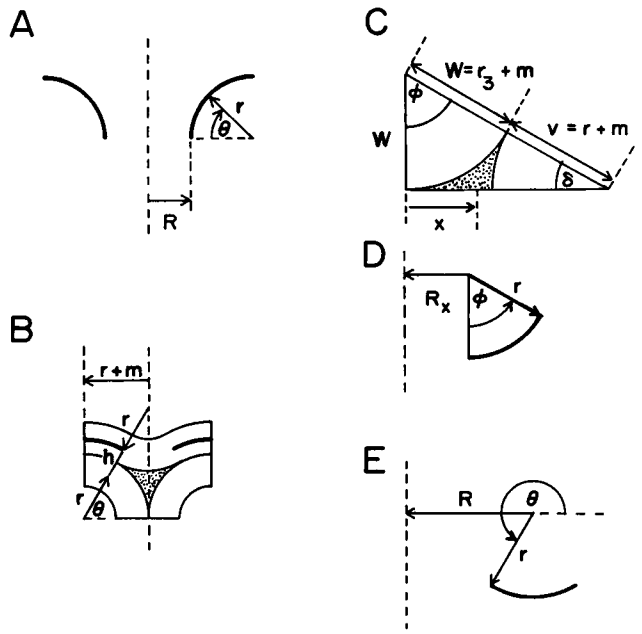

FIGURE 8 (*A*) A toroid of revolution is formed by rotating the arc of radius r around the dashed vertical axis. The exterior monolayers of the stalk and TMC have this geometry. (*B*) The surface formed at the margins of the *trans* monolayers overlying the ASVs in the stalk is obtained by rotating the arcs drawn in heavy lines about the dashed vertical axis. The stippled area represents an ASV. The lipid monolayers are outlined in light lines. (*C*) Location of the centroid of the TSV in a TMC. The cross-section of the TSV is stippled. The dashed vertical axis at left is the axis of the TMC. The lipid monolayers are outlined. (*D*) Radial expansion of the dimple in a TMC. The location of the diagrammed segment in the structure is the same as in *C*, except that a planar bilayer disk of radius R_x has been introduced into the center of the dimple. In Eq. A4, G_c is calculated for the surface obtained by rotating the arc of radius r around the dashed vertical axis at left. (*E*) Toroidal depression in the *trans* monolayers overlying the TSVs in an IMI. In Eq. A5, G_c is calculated for the surface obtained by rotating the arc of radius r around the dashed vertical axis at left, which would be the axis of the IMI.

curvature. The range of θ is $\pi/3 \le \theta \le \pi/2$. G_c for this surface is:

$$G_c = 2\pi k_m\left[\frac{1}{r+h} - C_0\right] \times \left[(r+m)\left(\theta - \frac{\pi}{3}\right) - 2(r+h)\left(\sin\theta - \frac{\sqrt{3}}{2}\right)\right] + \frac{\pi k_m}{aD}\left\{\ln\left[\frac{D\tan(\theta/2) + 1 - a}{D\tan(\theta/2) - 1 + a}\right] - \ln\left[\frac{(D/\sqrt{3}) + 1 - a}{(D/\sqrt{3}) - 1 + a}\right]\right\}, \quad \text{(A2)}$$

where $m = h/2$, $a = (r + h)/(r + m)$, and $D = (a^2 - 1)^{1/2}$. This expression is valid for $a > 1$. This energy is zero for $\theta = \pi/3$ ($\epsilon = \pi/6$; Fig. 2).

Dependence of TSV dimensions and centroid position on r and r_3

It can be shown that the cross-sectional area of a TSV is fairly insensitive to changes in the ratio of the radii of the monolayers comprising the different sides, so it is valid to use g_{tsv} evaluated at radius r_3 for the TMC (Eq. 6). For example, a 15% difference in r and r_3 at $r_3 = 2.3$ nm makes a ca. 6% difference in the cross-sectional area of the TSV. However, the position of the centroid of the TSV in the TMC is somewhat more sensitive. The locus of the centroid is where the perimeter of the TSV is evaluated. Refer to Fig. 8 *C*. The centroid position x is

$$x = \frac{AW^3 - Bv^3 - v^2[(W+v)\cos\delta - v][(\delta/2) - \cos\delta\cdot\sin\delta/2]}{CW^2 - v^2[\delta/2 - \sin\delta\cdot\cos\delta/2]}, \quad \text{(A3)}$$

where

$$A = \cos^3\phi/3 - \cos 2\phi - 1/12, \quad B = \delta/2 - \sin 2\delta/4 - \sin^3\delta/3,$$

$$C = \sin\phi - \sin\phi\cdot\frac{\cos\phi}{2} - \frac{\phi}{2}, \quad \phi = \arccos\left(\frac{W}{W+v}\right),$$

$$\delta = \pi/2 - \phi, \quad W = r_3 + m, \quad v = r + m.$$

Inner toroid of the radially expanding TMC

G_c for the surface depicted in Fig. 8 *D* is given by:

$$G_c = \frac{\pi k_m R_x}{r_3 a}\left\{\ln\left[\frac{\tan(\phi/2) + b - a}{\tan(\phi/2) + b + a}\right] - \ln\left(\frac{b-a}{b+a}\right)\right\} + 2\pi k_m[R_x C_0\phi + 2(1 + r_3 C_0)(1 - \cos\phi)], \quad \text{(A4)}$$

where

$$b = r_3/R_x, \quad a = (b^2 - 1)^{1/2},$$

and ϕ is as given in Eq. A3. This expression is valid for $R_x \le r$.

Toroidal depression in the *trans* monolayers of IMI

Refer to Fig. 8 *E*. Note that this expression diverges for angles that are multiples of π. For the *trans* monolayer depressions of an IMI, $4\pi/3 \le \theta \le 5\pi/3$, and $R = r + m$, where r is the marginal radius of the IMI (Fig. 3 *B*). G_c of this surface, with headgroups inside the toroid, is:

$$G_c = \frac{2\pi k_m R^2}{r(R^2 - r^2)^{1/2}}\arctan\left[\frac{(R^2 - r^2)^{1/2}\cdot\tan(\theta/2)}{R + r}\right]_{\theta_1}^{\theta_2} + 2\pi k_m RC_0(\theta_2 - \theta_1) + 4\pi k_m(1 + rC_0)(\sin\theta_2 - \sin\theta_1). \quad \text{(A5)}$$

Note that this expression is only valid for $R > r$.

I am particularly grateful to L. Chernomordik for several illuminating discussions, and I thank J. Seddon for a helpful discussion of Gaussian curvature elastic energies. I am also very grateful to S. Gruner and J. Bentz for comments on early versions of the manuscript, and to S. Gruner and M. Caffrey for sharing data in advance of publication.

REFERENCES

Andersson, S., S. T. Hyde, K. Larsson, and S. Lidin. 1988. Minimal surfaces and structures: from inorganic and metal crystals to cell membranes and biopolymers. *Chem. Rev.* 88:221–242.

Bentz, J. 1992. Intermediates and kinetics of membrane fusion. *Biophys. J.* 63:448–459.

Bentz, J. 1993. Viral Fusion Mechanisms. CRC Press, Boca Raton, FL.

Bentz, J., S. Nir, and J. Wilschut. 1983. Mass action kinetics of vesicle aggregation and fusion. *Colloids Surf.* 6:333–363.

Bentz, J., H. Ellens, M.-Z. Lai, and F. C. Szoka. 1985. On the correlation between H_{II} phase and the contact-induced destabilization of phosphatidylethanolamine-containing membranes. *Proc. Natl. Acad. Sci. USA.* 82:5742–5745.

Bentz, J., H. Ellens, and F. C. Szoka. 1987. Destabilization of phosphatidylethanolamine-containing liposomes: hexagonal phase and asymmetric membranes. *Biochemistry.* 26:2105–2116.

Bo, L., and R. E. Waugh. 1989. Determination of bilayer membrane bending stiffness by tether formation of giant, thin-walled vesicles. *Biophys. J.* 55:509–517.

Brown, P. M., and J. R. Silvius. 1989. Stability and fusion of lipid vesicles containing headgroup-modified analogues of phosphatidylethanolamine. *Biochim. Biophys. Acta.* 980:181–190.

Castellan, G. W. 1971. Physical Chemistry. 2nd ed. Addison-Wesley Publ. Co., Menlo Park, CA.

Chernomordik, L. V., M. M. Kozlov, G. B. Melikyan, I. G. Abidor, V. S. Markin, and Yu. A. Chizmadzhev. 1985. The shape of lipid molecules and monolayer membrane fusion. *Biochim. Biophys. Acta.* 812:643–655.

Chernomordik, L. V., G. B. Melikyan, and Yu. A. Chizmadzhev. 1987. Biomembrane fusion: a new concept derived from model studies using two interacting planar lipid bilayers. *Biochim. Biophys. Acta.* 906: 309–352.

Chernomordik, L. V., S. S. Vogel, A. Sokoloff, H. O. Onaran, E. A. Leikina, and J. Zimmerberg. 1993. Lysolipids reversibly inhibit Ca^{2+}-, GTP- and pH-dependent fusion of biological membranes. *FEBS Lett.* 318:71–76.

Devaux, P. F. 1991. Static and dynamic lipid asymmetry in cell membranes. *Biochemistry.* 30:1163–1173.

Düzgünes, N., J. Wilschut, R. Fraley, and D. Papahadjopoulos. 1981. Studies on the mechanism of membrane fusion. Role of head-group composition in calcium- and magnesium-induced fusion of mixed phospholipid vesicles. *Biochim. Biophys. Acta.* 642:182–195.

Düzgünes, N., J. Paiement, K. B. Freeman, N. G. Lopez, J. Wilschut, and D. Papahadjopoulos. 1984. Modulation of membrane fusion by inotropic and thermotropic phase transitions. *Biochemistry.* 23:3486–3494.

Düzgünes, N., and J. Bentz. 1988. Fluorescence assays for membrane fusion. *In* Spectroscopic Membrane Probes. Vol. 1. L. M. Loew, editor. CRC Press, Boca Raton, FL. 117–159.

Eastman, S. J., M. J. Hope, K. F. Wong, and P. R. Cullis. 1992. Influence of phospholipid asymmetry on fusion between large unilamellar vesicles. *Biochemistry.* 31:4262–4268.

Ellens, H., J. Bentz, and F. C. Szoka. 1986a. Destabilization of phosphatidylethanolamine liposomes at the hexagonal phase transition temperature. *Biochemistry.* 25:285–294.

Ellens, H., J. Bentz, and F. C. Szoka. 1986b. Fusion of phosphatidylethanolamine-containing liposomes and mechanism of the L_α-H_{II} phase transition. *Biochemistry.* 25:4141–4147.

Ellens, H., D. P. Siegel, D. Alford, P. L. Yeagle, L. Boni, L. J. Lis, P. J. Quinn, and J. Bentz. 1989. Membrane fusion and inverted phases. *Biochemistry.* 28:3692–3703.

Gruner, S. M. 1985. Intrinsic curvature hypothesis for biomembrane lipid composition: a role for nonbilayer lipids. *Proc. Natl. Acad. Sci. USA.* 82:3665–3669.

Gruner, S. M. 1989. Stability of lyotropic phases with curved interfaces. *J. Phys. Chem.* 93:7562–7570.

Gruner, S. M., V. A. Parsegian, and R. P. Rand. 1986. Directly measured deformation energy of phospholipid H_{II} hexagonal phases. *Faraday Discuss. Chem. Soc.* 81:29–37.

Gruner, S. M., M. W. Tate, G. L. Kirk, P. T. C. So, D. C. Turner, D. T. Keane, C. P. S. Tilcock, and P. R. Cullis. 1988. X-ray diffraction study of the polymorphic behavior of *N*-methylated dioleoylphosphatidyl-ethanolamine. *Biochemistry.* 27:2853–2866.

Guy, H. R., S. R. Durell, C. Schoch, and R. Blumenthal. 1992. Analyzing the fusion process of influenza hemagglutinin by mutagenesis and molecular modeling. *Biophys. J.* 62:113–115.

Helfrich, W. 1973. Elastic properties of lipid bilayers: theory and possible experiments. *Z. Naturforsch. Sect. C Biosci.* 28C:693–703.

Hui, S. W., T. P. Stewart, and L. T. Boni. 1982. Membrane fusion through point defects in bilayers. *Science (Washington, DC).* 212:921–923.

Keller, S. L., S. M. Bezrukov, S. M. Gruner, M. W. Tate, I. Vodyanoy, and V. A. Parsegian. 1993. Probability of alamethicin conductance states varies with nonlamellar tendency of bilayer phospholipids. *Biophys. J.* 65:23–27.

Kirk, G. L., S. M. Gruner, and D. L. Stein. 1984. A thermodynamic model of the lamellar to inverse hexagonal phase transition of lipid-water systems. *Biochemistry.* 23:1093–1102.

Kirk, G. L., and S. M. Gruner. 1985. Lyotropic effects of alkanes and headgroup composition on the L_α-H_{II} lipid liquid crystalline phase transition: hydrocarbon packing *vs.* intrinsic curvature. *J. Physique (Paris).* 46: 761–769.

Kozlov, M. M., S. L. Leikin, L. V. Chernomordik, V. S. Markin, and Yu. A. Chizmadzhev. 1989. Stalk mechanism of membrane fusion. Intermixing of aqueous contents. *Eur. Biophys. J.* 17:121–129.

Kozlov, M. M., and M. Winterhalter. 1991. Elastic moduli and neutral surface for strongly curved monolayers. Analysis of experimental results. *J. Physiol. (Paris).* 1:1085–1100.

Leikin, S. L., M. M. Kozlov, L. V. Chernomordik, V. S. Markin, and Yu. A. Chizmadzhev. 1987. Membrane fusion: overcoming of the hydration barrier and local restructuring. *J. Theor. Biol.* 129:411–425.

Lentz, B. R., G. F. McIntyre, D. J. Parks, J. C. Yates, and D. Massenburg. 1992. Bilayer curvature and certain amphipaths promote poly(ethylene glycol)-induced fusion of dipalmitoylphosphatidylcholine unilamellar vesicles. *Biochemistry.* 31:2643–2653.

Lewis, R. A. H., D. A. Mannock, R. N. McElhaney, D. C. Turner, and S. M. Gruner. 1989. Effect of fatty acyl chain length and structure on the lamellar gel to liquid crystalline and lamellar to reversed hexagonal phase transitions of aqueous phosphatidylethanolamine dispersions. *Biochemistry.* 28:541–548.

Lindblom, G., and L. Rilfors. 1989. Cubic phases and isotropic structures formed by lipids - possible biological relevance. *Biochim. Biophys. Acta.* 988:221–256.

Markin, V. S., M. M. Kozlov, and V. L. Borovjagin. 1984. On the theory of membrane fusion. The stalk mechanism. *Gen. Physiol. Biophys.* 5: 361–377.

Marsh, D. 1990. Handbook of Lipid Bilayers. CRC Press, Boca Raton, FL.

Rand, R. P., N. L. Fuller, S. M. Gruner, and V. A. Parsegian. 1990. Membrane curvature, lipid segregation, and structural transitions for phospholipids under dual solvent stress. *Biochemistry.* 29:76–87.

Ruigrok, R. W. H., E. A. Hewat, and R. H. Wade. 1992. Low pH deforms the influenza virus envelope. *J. Gen. Virol.* 73:995–998.

Schneider, M. B., J. T. Jenkins, and W. W. Webb. 1984. Thermal fluctuations of large quasi-spherical bimolecular phospholipid vesicles. *J. Physique (Paris).* 45:1457–1472.

Seddon, J. M. 1990. Structure of the inverted hexagonal (H_{II}) phase, and non-lamellar phase transitions in lipids. *Biochim. Biophys. Acta.* 1031: 1–69.

Siegel, D. P. 1984. Inverted micellar structures in bilayer membranes: formation rates and half-lives. *Biophys. J.* 45:399–420.

Siegel, D. P. 1986a. Inverted micellar intermediates and the transitions between lamellar, inverted hexagonal, and cubic lipid phases. I. Mechanism of the L -to-H_{II} phase transition. *Biophys. J.* 49:1155–1170.

Siegel, D. P. 1986b. Inverted micellar intermediates and the transitions between lamellar, inverted hexagonal, and cubic lipid phases. II. Implications for membrane-membrane interactions and membrane fusion. *Biophys. J.* 49: 1171–1183.

Siegel, D. P. 1986c. Inverted micellar intermediates and the transitions between lamellar, inverted hexagonal, and cubic lipid phases. III. Formation of isotropic and inverted cubic phases and membrane fusion via intermediates in transitions between L_α and H_{II} phases. *Chem. Phys. Lipids.* 42:279–301.

Siegel, D. P. 1993. Modeling protein-induced fusion mechanisms: insights from the relative stability of lipidic structures. *In* Viral Fusion Mechanisms. J. Bentz, editor. CRC Press, Boca Raton, FL. 475–512.

Siegel, D. P., J. Banschbach, D. Alford, H. Ellens, L. J. Lis, P. J. Quinn, P. L. Yeagle, and J. Bentz. 1989a. Physiological levels of diacylglcyerols in phospholipid membranes induce membrane fusion and stabilize inverted phases. *Biochemistry.* 28:3703–3709.

Siegel, D. P., J. Banschbach, and P. L. Yeagle. 1989b. Stabilization of H_{II} phases by low levels of diglycerides and alkanes: an NMR, calorimetric, and X-ray diffraction study. *Biochemistry.* 28:5010–5019.

Siegel, D. P., and J. L. Banschbach. 1990. Lamellar/inverted cubic (L_α/Q_{II}) phase transition in *N*-methylated dioleoylphosphatidyl-ethanolamine. *Biochemistry.* 29:5975–5981.

Silvius, J. R., and J. Gagné. 1984. Lipid phase behavior and calcium-induced fusion of phosphatidylethanolamine-phosphatidylserine vesicles. Calorimetric and fusion studies. *Biochemistry.* 23:3232–3240.

Sjölund, M., G. Lindblom, L. Rilfors, and G. Avidson. 1987. Hydrophobic molecules in lecithin-water systems. I. Formation of reversed hexagonal phases at high and low water contents. *Biophys. J.* 52:145–153.

Sjölund, M., L. Rilfors, and G. Lindblom. 1989. Reversed hexagonal phase formation in lecithin-alkane-water systems with different acyl chain unsaturation and alkane length. *Biochemistry*. 28: 1323–1329.

Small, D. M. 1986. The Physical Chemistry of Lipids. *In* The Handbook of Lipid Research. Vol. 4. D. J. Hanahan, series editor. Plenum Press, New York.

Stamatatos, L., and J. R. Silvius. 1987. Effects of cholesterol on the divalent cation-mediated interactions of vesicles containing amino and choline phospholipids. *Biochim. Biophys. Acta*. 905:81–90.

Tate, M. W., and S. M. Gruner. 1987. Lipid polymorphism of mixtures of dioleoylphosphatidylethanolamine and saturated and monounsaturated phosphatidylcholines of various chain lengths. *Biochemistry*. 26:231–236.

Tate, M. W., and S. M. Gruner. 1989. Temperature dependence of the structural dimensions of the inverted hexagonal (H_{II}) phase of phosphatidylethanolamine-containing membranes. *Biochemistry*. 28:4245–4253.

Tate, M. W., E. F. Eikenberry, D. C. Turner, E. Shyamsunder, and S. M. Gruner. 1991. Nonbilayer phases of membrane lipids. *Chem. Phys. Lipids*. 57:147–164.

Turner, D. C. Structural investigations of the inverted hexagonal and inverted cubic phases in lipid-water systems. Ph.D. thesis. Princeton University, Princeton, NJ. 230 pp.

Turner, D. C., and S. M. Gruner. 1992. X-ray reconstruction of the inverted hexagonal (H_{II}) phase in lipid-water systems. *Biochemistry*. 31: 1340–1355.

Verkleij, A. J. 1984. Lipidic intramembranous particles. *Biochim. Biophys. Acta*. 779:43–63.

Verkleij, A. J., C. J. A. VanEchteld, W. J. Gerritsen, P. R. Cullis, and B. DeKruijff. 1980. The lipidic particle as an intermediate structure in membrane fusion processes and bilayer to hexagonal H_{II} transitions. *Biochim. Biophys. Acta*. 600:620–624.

Walter, A., and D. P. Siegel. 1993. Divalent cation-induced lipid mixing between phosphatidylserine liposomes studied by stopped-flow fluorescence measurements: effects of temperature, comparison of barium and calcium, and perturbation by DPX. *Biochemistry*. 32:3271–3281.

White, J. M. 1992. Membrane fusion. *Science (Washington, DC)*. 258: 917–924.

Wilschut, J., J. Scholma, S. J. Eastman, M. J. Hope, and P. R. Cullis. 1992. Ca^{2+}-induced fusion of phospholipid vesicles containing free fatty acids: modulation by transmembrane pH gradients. *Biochemistry*. 31: 2629–2636.